

13. E. W. Myers *et al.*, *Science* **287**, 2196 (2000).
 14. J. C. Venter *et al.*, *Science* **280**, 1540 (1998).
 15. M. D. Adams, J. J. Sekelsky, *Nat. Rev. Genet.* **3**, 189 (2002).
 16. U. S. Eggert *et al.*, *PLoS Biol.* **2**, e379 (2004).
 17. R. Dasgupta, N. Perrimon, *Oncogene* **23**, 8359 (2004).
 18. M. Boutros *et al.*, *Science* **303**, 832 (2004).
 19. A. A. Kiger *et al.*, *J. Biol. Chem.* **278**, 27 (2003).
 20. V. Korinek *et al.*, *Nat. Genet.* **19**, 379 (1998).
 21. V. Korinek *et al.*, *Mol. Cell. Biol.* **18**, 1248 (1998).
 22. A. S. Miller *et al.*, *In Vitro Cell. Dev. Biol. Anim.* **36**, 180 (2000).
 23. D. J. Peel, M. J. Milner, *Tissue Cell* **22**, 749 (1990).
 24. S. Yanagawa, J. S. Lee, A. Ishimoto, *J. Biol. Chem.* **273**, 32353 (1998).
 25. S. Yanagawa *et al.*, *EMBO J.* **21**, 1733 (2002).
 26. S. Yanagawa, F. van Leeuwen, A. Wodarz, J. Klingensmith, R. Nusse, *Genes Dev.* **9**, 1087 (1995).
 27. H. Matsubayashi *et al.*, *Mol. Cell. Biol.* **24**, 2012 (2004).
 28. Materials and methods are available as supporting material on Science Online.
 29. L. Schweizer, H. Varmus, *BMC Cell Biol.* **4**, 4 (2003).
 30. www.flyrnai.org.
 31. A. Schlesinger, A. Kiger, N. Perrimon, B. Z. Shilo, *Dev. Cell* **7**, 535 (2004).
 32. www.sdbonline.org/fly/segment/wingless1.htm
 33. www.sdbonline.org/fly/segment/arrow1.htm
 34. www.sdbonline.org/fly/neural/frizzled.htm
 35. www.sdbonline.org/fly/segment/naked1.htm
 36. www.sdbonline.org/fly/segment/axin1.htm
 37. www.sdbonline.org/fly/dbzhnsky/slimb1.htm
 38. www.sdbonline.org/fly/segment/dishevel.htm
 39. www.sdbonline.org/fly/segment/armadillo.htm
 40. www.sdbonline.org/fly/segment/pangolin1.htm
 41. www.sdbonline.org/fly/hjmuller/crebbp1.htm
 42. www.sdbonline.org/fly/segment/pygopus1.htm
 43. www.sdbonline.org/fly/segment/legless1.htm
 44. D. Sinner, S. Rankin, M. Lee, A. M. Zorn, *Development* **131**, 3069 (2004).
 45. A. Bauer *et al.*, *EMBO J.* **19**, 6121 (2000).
 46. A. Bauer, O. Huber, R. Kemler, *Proc. Natl. Acad. Sci. U.S.A.* **95**, 14787 (1998).
 47. C. Jung, R. S. Kim, S. J. Lee, C. Wang, M. H. Jeng, *Cancer Res.* **64**, 3046 (2004).
 48. M. C. Ramel, A. C. Lekven, *Development* **131**, 3991 (2004).
 49. K. Tamai *et al.*, *Mol. Cell* **13**, 149 (2004).
 50. M. Hatzfeld, *Int. Rev. Cytol.* **186**, 179 (1999).
 51. S. Greaves, B. Sanson, P. White, J. P. Vincent, *Genetics* **153**, 1753 (1999).
 52. A. H. Tang, T. P. Neufeld, G. M. Rubin, H. A. Muller, *Development* **128**, 801 (2001).
 53. M. A. Su, R. G. Wisotzkey, S. J. Newfeld, *Genetics* **157**, 717 (2001).
 54. R. DasGupta, N. Perrimon, unpublished data.
 55. G. H. Baeg, E. M. Selva, R. M. Goodman, R. Dasgupta, N. Perrimon, *Dev. Biol.* **276**, 89 (2004).
 56. K. A. Wharton Jr., G. Zimmermann, R. Rousset, M. P. Scott, *Dev. Biol.* **234**, 93 (2001).
 57. R. Rousset *et al.*, *Genes Dev.* **15**, 658 (2001).
 58. J. L. Seachrist, S. S. Ferguson, *Life Sci.* **74**, 225 (2003).
 59. J. L. Rosenfeld, B. J. Knoll, R. H. Moore, *Receptors Channels* **8**, 87 (2002).
 60. M. Gonzalez-Gaitan, *Nat. Rev. Mol. Cell Biol.* **4**, 213 (2003).
 61. M. Miaczynska *et al.*, *Cell* **116**, 445 (2004).
 62. A. Benmerah, *Curr. Biol.* **14**, R314 (2004).
 63. K. M. Cadigan, M. P. Fish, E. J. Rulifson, R. Nusse, *Cell* **93**, 767 (1998).
 64. R. T. Moon, A. Kaykas, unpublished observations.
 65. G. M. Kelly, P. Greenstein, D. F. Erezylmaz, R. T. Moon, *Development* **121**, 1787 (1995).
 66. R. T. Moon, A. D. Kohn, G. V. De Ferrari, A. Kaykas, *Nat. Rev. Genet.* **5**, 691 (2004).
 67. http://superfly.ucsd.edu/homophila/.
 68. We thank H. Bellen (Senseless antibody) and M. Gonzalez-Gaitan (UAS-Rab5 flies) for reagents and B. Mathey-Prevot, K. Nybakken, P. Bradley, S. Raghavan, A. Friedman, and H. Agaisse for lively discussion and critical comments on the manuscript. We thank D. J. Grau for assistance with Rab5 expression constructs. We also thank members of the *Drosophila* RNAi Screening Center (DRSC) and Institute of Chemistry and Cell Biology (ICCB) for their assistance. We thank G. Weidinger for assistance with zebrafish experiments and J. Tee for assistance with construction of siRNA and cDNA expression constructs. R.D. was supported by fellowships from the "Breast Cancer Research Foundation" of the U.S. Army. N.P. and R.T.M. are investigators, and A.K. is an associate, of the Howard Hughes Medical Institute.

Supporting Online Material
 www.sciencemag.org/cgi/content/full/1109374/DC1
 Materials and Methods
 Figs. S1 to S4
 Tables S1 to S5
 References and Notes

4 January 2005; accepted 2 March 2005
 Published online 7 April 2005;
 10.1126/science.1109374
 Include this information when citing this paper.

MicroRNAs Regulate Brain Morphogenesis in Zebrafish

Antonio J. Giraldez,^{1*} Ryan M. Cinalli,¹ Margaret E. Glasner,^{2,†}
 Anton J. Enright,³ J. Michael Thomson,⁴ Scott Baskerville,²
 Scott M. Hammond,⁴ David P. Bartel,² Alexander F. Schier^{1*}

MicroRNAs (miRNAs) are small RNAs that regulate gene expression posttranscriptionally. To block all miRNA formation in zebrafish, we generated maternal-zygotic *dicer* (*MZdicer*) mutants that disrupt the Dicer ribonuclease III and double-stranded RNA-binding domains. Mutant embryos do not process precursor miRNAs into mature miRNAs, but injection of preprocessed miRNAs restores gene silencing, indicating that the disrupted domains are dispensable for later steps in silencing. *MZdicer* mutants undergo axis formation and differentiate multiple cell types but display abnormal morphogenesis during gastrulation, brain formation, somitogenesis, and heart development. Injection of miR-430 miRNAs rescues the brain defects in *MZdicer* mutants, revealing essential roles for miRNAs during morphogenesis.

MicroRNAs are evolutionarily conserved small non-protein-coding RNA gene products that regulate gene expression at the posttranscriptional level (1–3). In animals, mature miRNAs are ~22 nucleotides (nt) long and are generated from a primary transcript (termed pri-miRNA) through sequential processing by nucleases belonging to the ribonuclease III (RNaseIII) family. Initially, Droscha cleaves the pri-miRNA and excises a stem-loop precursor of ~70 nt (termed pre-miRNA), which is then cleaved by Dicer (4–7). One strand of the processed duplex is incorporated into a silencing complex and guides it to target sequences (1, 3). This re-

sults in the cleavage of target mRNAs and/or the inhibition of their productive translation (1–3).

Several hundred vertebrate miRNAs and several thousand miRNA targets have been predicted or identified, but little is known about miRNA function during development (1, 2, 8, 9). Clues to vertebrate miRNA function have come from several approaches, including expression analyses (1–3, 10–12), computational prediction of miRNA targets (8, 13–15), experimental support of predicted targets (13, 14, 16, 17), cell culture studies (16), and gain-of-function approaches (18). These studies have led to the suggestions that

vertebrate miRNAs might be involved in processes such as stem cell maintenance (12, 19) or cell fate determination (17, 18, 20); however, no loss-of-function analysis has assigned a role for a particular miRNA or miRNA family *in vivo*, and it has been unclear how widespread the role of miRNAs is during vertebrate embryogenesis.

One approach to reveal the global role of vertebrate miRNAs is to abolish the generation of mature miRNAs with the use of *dicer* mutants. For example, *dicer* mutant embryonic stem cells fail to differentiate *in vivo* and *in vitro* (20), and *dicer* mutant mice die before axis formation (19), suggesting that mature miRNAs (or other Dicer products) are essential for early mammalian development. In zebrafish, maternal *dicer* activity has hampered the analysis of the single *dicer* gene. Mutants for the zygotic function of *dicer* (*Zdicer*) retain pre-miRNA processing activity up to 10 days postfertilization,

¹Developmental Genetics Program, Skirball Institute of Biomolecular Medicine and Department of Cell Biology, New York University School of Medicine, New York, NY 10016, USA. ²Whitehead Institute for Biomedical Research and Department of Biology, Massachusetts Institute of Technology, 9 Cambridge Center, Cambridge, MA 02142, USA. ³Wellcome Trust Sanger Institute, Hinxton, Cambridge CB10 1SA, UK. ⁴Department of Cell and Developmental Biology, Lineberger Comprehensive Cancer Center, University of North Carolina, Chapel Hill, NC 27599, USA.

*To whom correspondence should be addressed. E-mail: schier@saturn.med.nyu.edu (A.F.S.); giraldez@saturn.med.nyu.edu (A.J.G.)

†Present address: Department of Pharmaceutical Chemistry, University of California, San Francisco, 600 16th Street, Box 2240, San Francisco, CA 94143–2240, USA.

presumably because of maternally contributed *dicer* (21). *Zdicer* mutants have no obvious defects other than a developmental delay at 7 to 10 days postfertilization, a stage when embryogenesis and major steps of organogenesis have been achieved (21). Hence, the global role of miRNAs during vertebrate embryogenesis is unknown. In light of these observations, we decided to generate zebrafish embryos that lack both maternal and zygotic *dicer* activity.

Generation of Maternal-Zygotic *dicer* Mutants

To eliminate all maternal contribution in *dicer* mutants, we took advantage of the germ line replacement technique (22). Wild-type zebrafish embryos depleted of their germ cells served as hosts for germ cells from homozygous *dicer* mutant donor embryos (fig. S1). The resulting fish were fertile even though they had a germ line that was exclusively con-

stituted by mutant donor cells. As donors, we used *dicer*^{hu715/hu715} mutants, an allele that codes for a truncated Dicer protein that disrupts the RNaseIII and double-stranded RNA (dsRNA)-binding domains (21). Intercrossing of fish that had a *dicer* mutant germ line generated embryos that were maternal-zygotic mutant for *dicer* (MZ*dicer*). In marked contrast to *Zdicer* mutants, MZ*dicer* embryos did not generate mature miRNAs and displayed severe morphogenesis defects.

Loss of pre-miRNA Processing in MZ*dicer* Mutants

Similar to other model systems, wild-type zebrafish embryos generate mature miRNAs from endogenous (21, 23) or exogenously provided pri-miRNAs, resulting in the post-transcriptional repression of reporter genes (fig. S2). miRNAs induce the cleavage of reporter RNAs with perfectly complementary target sites (PT) in the 3' untranslated region

(3'UTR), whereas imperfectly complementary sites (IPT) result in the noneffective translation of reporter mRNAs (24) (fig. S3). Previous biochemical and genetic studies have shown that Dicer is required for the generation of mature miRNAs (4, 5). To determine whether MZ*dicer* embryos lack mature miRNAs, we first hybridized total RNA from 1-day-old zebrafish embryos to a microarray of probes for 120 different zebrafish mature miRNAs (10). Although such arrays are susceptible to cross-hybridization artifacts, we observed a marked reduction of signals in MZ*dicer* mutants compared with wild-type embryos and zygotic *dicer* mutants (Fig. 1A). Of the 120 miRNA probes, 59, 35, and 9 gave a detectable signal in wild-type embryos, *Zdicer* mutants, and MZ*dicer* mutants, respectively. To test for the presence of mature miRNAs more specifically, we performed Northern blot analyses. We found that of eight miRNAs present in wild-type embryos, none was detected in MZ*dicer* mutants (Fig. 1B) (25). In most of these cases, the lack of processing resulted in an accumulation of the pre-miRNA (Fig. 1B). Northern analyses also suggested that the nine positive signals on the microarray probed with MZ*dicer* RNA are unlikely to be due to mature miRNAs. First, we found that one miRNA (miR-206) is processed in wild-type but not mutant embryos (Fig. 1B). Second, two miRNAs (miR-223 and miR-122a) were detectable neither in wild-type embryos nor MZ*dicer* mutants (Fig. 1B) (25). These results suggested that mature miRNAs were not generated in MZ*dicer* mutants.

As an additional assay for miRNA maturation in MZ*dicer* mutants, we examined the response of a green fluorescent protein (GFP) reporter (3xPT-miR-430b) containing target sites for members of the miR-430 family of

Fig. 1. MZ*dicer* mutants lack mature miRNAs. (A) miRNA array expression data from MZ*dicer*, *Zdicer*, and wild-type (wt) embryos at 32, 28, and 28 hpf, respectively. The range of signal was from -100-fold to 0 to +100-fold. Yellow denotes high signal and blue denotes low signal. The asterisks highlight miRNAs whose expression was also analyzed by Northern blot. (B) Northern blot analysis of different miRNAs in MZ*dicer* mutants (32 hpf) and wild-type embryos (28 hpf).

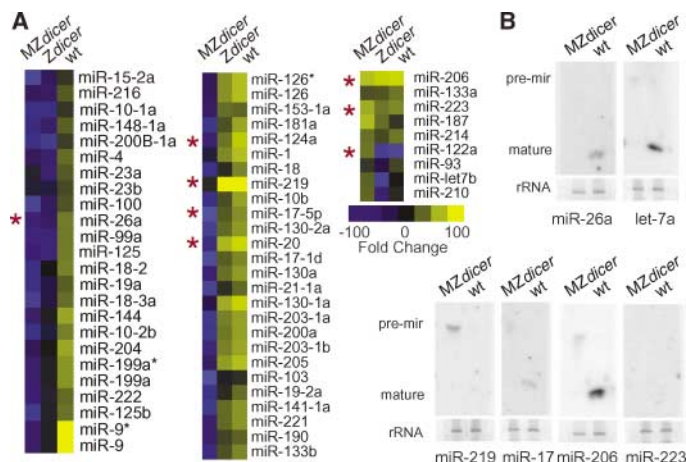
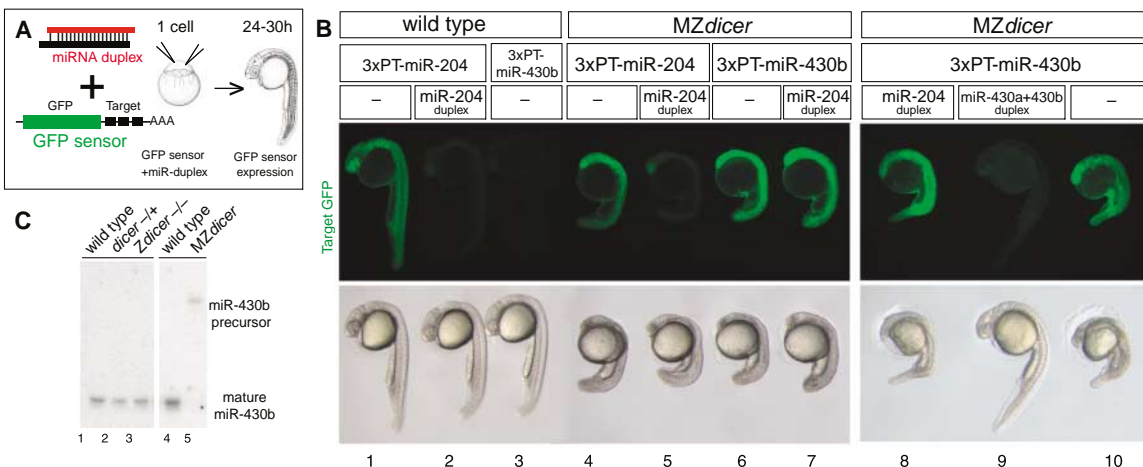


Fig. 2. Silencing activity of miRNA duplexes but not pri-miRNAs in MZ*dicer*. (A and B) Coinjection of miRNA duplexes (miR-204, miR-430a, or miR-430b) with GFP sensors that contain the coding sequence of GFP and three (3x) perfect target (PT) sites for the different miRNAs. See figs. S2 and S3 for details. (A) Schematic representation of the experimental set up. (B) Coinjection of GFP sensors with buffer (-) or miR duplexes into wild-type embryos and MZ*dicer* mutants. Fluorescent microscopy shows GFP target expression (green) at 24 to 30 hpf. Bright-field image of embryos is shown below. The specific silencing of the targets can be identified by their corresponding miRNA duplexes in wild-type and MZ*dicer* embryos. Endogenous miR-430 repressed the



expression of its GFP sensor in wild-type embryos but not in MZ*dicer* mutants. (C) Northern blot analysis of endogenous miR-430b in wild-type and MZ*dicer* embryos, showing the accumulation of the miR-430b precursor and absence of the mature form of this miRNA in MZ*dicer* embryos.

miRNAs (Fig. 2A). These miRNAs are transcribed at high levels in the embryo and silence reporter expression in wild-type embryos (Fig. 2, B and C). In contrast, the reporter is not silenced in *MZdicer* mutants, consistent with the lack of mature miRNAs (Fig. 2, B and C). We also injected a pri-miRNA (pri-miR-1) and followed its processing. Whereas pri-miR-1 mRNA was processed into mature miR-1 in wild-type embryos, no mature miR-1 was detected in *MZdicer* embryos (fig. S4). Moreover, reporter genes containing perfect or imperfect targets for miR-1 were no longer silenced in *MZdicer* mutants by pri-miR-1 injection (fig. S4). Taken together, these results indicate that *MZdicer* mutants do not process endogenous and exogenously provided pre-miRNAs and thus are devoid of mature miRNAs.

miRNA Duplexes Are Active in *MZdicer* Mutants

Injection of synthetic miRNA duplexes into wild-type zebrafish embryos initiates the effector step of RNA silencing and leads to the down-regulation of GFP reporters that contain complementary target sequences (24). Because recent studies have implicated Dicer in the assembly and function of the silencing complex (26–30), we analyzed the ability of exogenously provided miRNA duplexes to repress target expression in *MZdicer* mutants.

Wild-type and *MZdicer* mutant embryos were injected with GFP sensors for three different miRNAs and with either complementary or unrelated miRNA duplexes (Fig. 2, A and B, and fig. S4). We found that miRNA duplexes specifically repressed expression of their cognate targets in both wild-type and *MZdicer* mutant embryos (Fig. 2B and fig. S4). These results show that miRNAs can be incorporated into active silencing complexes in *MZdicer* mutants, indicating that the RNaseIII and dsRNA-binding domains of Dicer are not required for loading into the complex and subsequent silencing activity.

Dicer Is Essential for Embryonic Morphogenesis but Not Axis Formation

The absence of mature miRNAs in *MZdicer* mutants allowed us to determine their global requirement during early zebrafish development. The *MZdicer* phenotype notably differs from that of *Zdicer* mutants, which are indistinguishable from wild-type embryos during these stages (21) (Fig. 3, A to C). Morphological analysis during the first 5 days of development revealed that axis formation and the regionalization of *MZdicer* mutants were intact (Fig. 3C). Major subregions and cell types were present, ranging from forebrain, eye, midbrain, hindbrain, ear, pigment cells, and spinal cord to hatching gland, heart, notochord, somites, and blood (Fig. 3C and figs. S5 and S9).

In contrast, morphogenetic processes during gastrulation, somitogenesis, and heart and brain development were severely affected (Fig. 3, C and E to G, and figs. S5 and S10). *MZdicer* mutants also developed more slowly than wild-type embryos, with 3 to 4 hours of delay within the first 24 hours of development (fig. S5) (31).

Gastrulation. During zebrafish gastrulation, four concomitant cell rearrangements take place: (i) epiboly (spreading of the embryo over the yolk), (ii) internalization (formation of mesodermal and endodermal germ layers), (iii) convergence (movement of cells toward the dorsal side), and (iv) extension (lengthening of the embryo) (Fig. 3, E to G). *MZdicer* mutants failed to coordinate epiboly and internalization (Fig. 3E). This resulted in mutant embryos that had undergone prechordal plate migration corresponding to 80% epiboly in wild-type embryos, yet epiboly movements were delayed to a stage equivalent to 50 to 60% epiboly (Fig. 3E). *MZdicer* embryos also displayed a reduced extension of the axis, resulting in a shortening of the embryo and an accumulation of cells in the head region (Fig. 3, F and G). Later during development, *MZdicer* mutants had a reduced posterior yolk extension (fig. S5).

Neural development. Neurulation was severely affected in *MZdicer* embryos. The mutant neural plate gave rise to the neural rod, but the subsequent formation of the neurocoel and neural tube was notably impaired (Fig. 4, A, B,

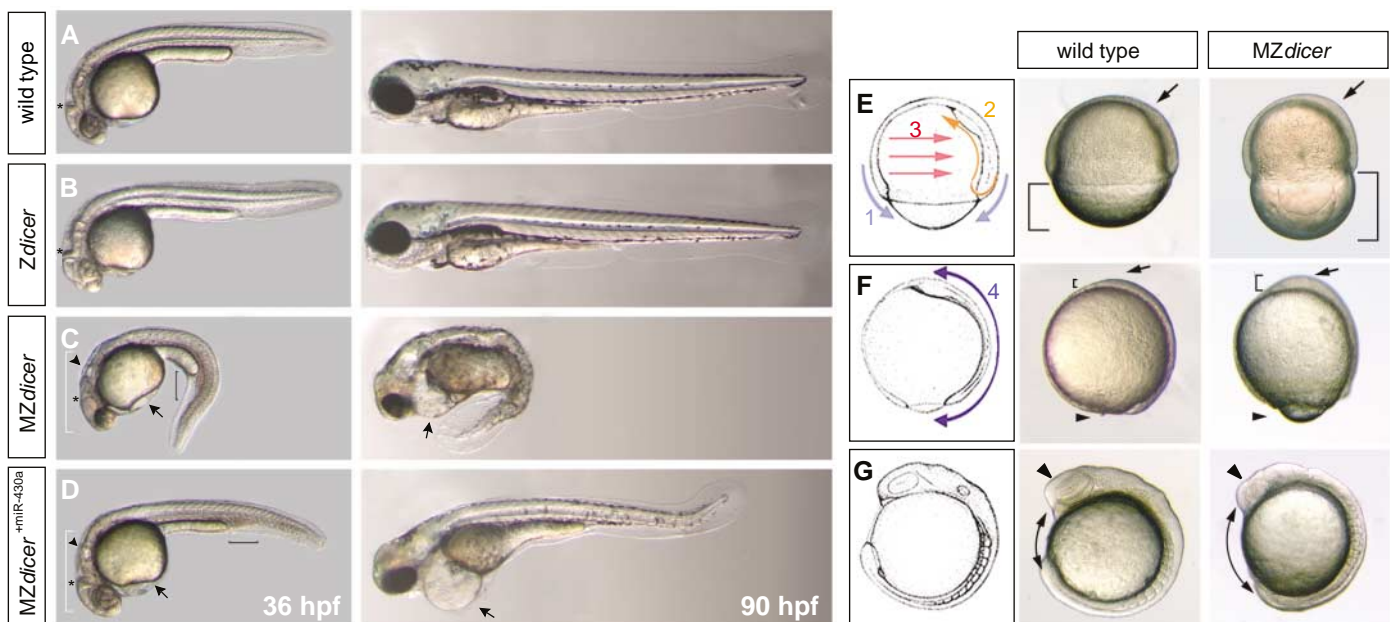


Fig. 3. Morphogenesis defects in *MZdicer* mutants. Compared with wild-type embryos (A), *Zdicer* mutants (B) have no morphological defects at 36 and 90 hpf. (C) *MZdicer* mutants display morphogenesis defects. This phenotype is fully penetrant and expressive. (D) *MZdicer* injected at the one cell stage with miR-430a duplex. Brain morphogenesis (white bracket), and the midbrain-hindbrain boundary (*) are rescued, and trunk morphology and somite boundary formation are partially rescued. Phenotypes that are not rescued include the lack of blood circulation (black bracket), heart edema (arrow), and defective ear development (arrowhead). (E to G) (Left) Scheme representing the cell movements (arrows) during gastrulation in

zebrafish: (1) epiboly, (2) internalization, (3) convergence, and (4) extension; (middle) wild-type embryo; (right) *MZdicer* mutants. (E) Embryos at 80% epiboly stage; arrow shows the similar extent of prechordal plate extension in wild-type embryos and *MZdicer* mutants; bracket shows a reduced extent in epiboly in *MZdicer* mutants compared with wild-type embryos. (F) Tail bud stage. Note the accumulation of cells in the region of the anterior axial mesendoderm (*MZdicer*, arrow and bracket). (G) Nine-somite stage. Note the abnormal development of the optic primordium (*MZdicer*, arrowhead) and reduction in axis extension that results in a shorter embryo (*MZdicer*, double arrow).

E, and F, and fig. S5). The formation of the brain ventricles was severely reduced. In wild-type embryos, several constrictions subdivide the brain into distinct regions. These constrictions did not form in *MZdicer* mutants. For example, the midbrain-hindbrain boundary that is very prominent in wild-type embryos did not form in *MZdicer* mutants (Fig. 4, B and arrowhead in F, and fig. S5). In addition, retinal development was affected (Fig. 4, A and B). Defects in the spinal cord were manifested by a rudimentary neurocoel and a reduction of the floor plate in the trunk (fig. S5).

Despite the gross morphological malformations of the nervous system, gene expression analysis suggested that anterior-posterior and dorsal-ventral patterning were not severely disrupted (fig. S6). Analysis of anterior-posterior and dorsal-ventral markers revealed normal specification of the optic stalk, forebrain, midbrain-hindbrain boundary, otic vesicles, hindbrain rhombomeres, and the dorsal and ventral neural tube.

Analysis of neuronal differentiation and axonal markers, with the use of HuC and HNK antibodies, revealed mispositioned trigeminal sensory neurons adjacent to the eye (fig. S7). In addition, we observed defasciculation of the postoptic commissure in *MZdicer* embryos (fig. S7). In the hindbrain, multiple neurons project longitudinal axons anteriorly and posteriorly and form a ladder-like structure on each side of the midline. This scaffold was disrupted and defasciculated in *MZdicer* mutants, but longitudinal axonal projections were established (fig. S7). In addition, touch-induced escape behavior was severely diminished in *MZdicer* mutants (fig. S8). Taken together, these results indicate that early patterning and fate specification in the embryonic nervous system are largely unaffected by lack of miRNAs. In contrast, normal brain morphogenesis and neural differentiation and function require Dicer activity.

Nonneural development. During somitogenesis, the paraxial mesoderm becomes segmented. *MZdicer* embryos formed normally spaced somites and expressed the muscle marker *myoD* similar to wild-type embryos (fig. S9). Later in development, the somites acquired a chevron shape in wild-type embryos but formed irregular boundaries in *MZdicer* mutants (fig. S5). Endothelial and hematopoietic precursor cells were present as judged from the expression of the markers *fli-1* and *scl*, respectively, but endocardial *fli-1* expression was reduced and blood circulation disrupted in *MZdicer* mutants (fig. S9). Analysis of the markers *pax2a*, *GFP-nanos-3'UTR*, *fkdl*, *cmlc2*, and *fkdl2* revealed that pronephros, germ cells, endoderm, cardiomyocytes, and liver cells, respectively, were specified (fig. S6) (25). *MZdicer* mutants had contractile cardiomyocytes but the two chambers characteristic of the wild-type heart did not form; instead, a tu-

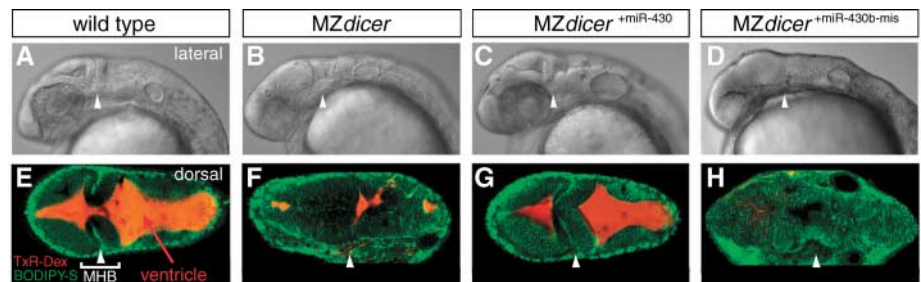


Fig. 4. miR-430 miRNAs rescue brain morphogenesis in *MZdicer* embryos. (A to D) Differential interference contrast (DIC) images of wild-type embryos (A), *MZdicer* mutants (B), *MZdicer* mutants injected with miR-430 duplex (*MZdicer*^{+miR-430}) (C), and *MZdicer* mutants injected with miR-430b-mis duplex (*MZdicer*^{+miR-430b-mis}) (D) that contains two mismatches in the seed of miR-430b. (E to H) Confocal dorsal view of embryos with the same genotype as in (A) to (D). Cell membranes were labeled in green (BODIPY) and the brain ventricles were labeled in red by injection of Texas-Red dextran into the brain. Wild-type embryos displayed the characteristic fold of the midbrain-hindbrain boundary (MHB) (arrowhead) and have brain ventricles (red) (E). *MZdicer* mutants do not form a midbrain-hindbrain boundary, lack normal brain ventricles, and display defects during eye development. [(C) and (G)] Injection of *MZdicer* mutants with the miR-430 duplex rescued brain development, including the midbrain-hindbrain boundary (arrowhead) and ventricle formation. Most (84%) of the embryos were rescued ($n = 104$). Eye development was also partially rescued. [(D) and (H)] Injection of the miR-430b-mis duplex, which contains two mismatches in the 5' seed, did not rescue these defects (0% rescued, $n = 50$).

bular heart and pericardial edema developed (fig. S10).

Taken together, these results indicated that *MZdicer* mutant embryos were patterned correctly and had multiple specified cell types but underwent abnormal morphogenesis, in particular during neural development and organogenesis.

The miR-430 miRNA Family

To identify miRNAs that might play important roles during early zebrafish development, we cloned small RNAs (~18 to 28 nt) from eight developmental stages between fertilization and 48 hours of development (32). These experiments identified miR-430a, miR-430b, and miR-430c as three highly expressed miRNAs, as well as several related species, miR-430d to miR-430h, which were expressed at lower levels (Fig. 5, A and B). The miR-430 family members each had the same sequence at nucleotides 2 to 8, which is known as the “seed” and has been shown to be the miRNA segment most important for target recognition (8, 13, 24, 33). The family members also have strong homology in their 3' region, but differ in their central and terminal nucleotides. Mapping of the miR-430 family to the zebrafish genome revealed a locus composed of multiple copies of the miR-430a,c,b triplet, with more than 90 copies of the miRNAs within 120 kb (Fig. 5C). miRNA genes are sometimes observed in clusters of about two to seven, which are frequently transcribed as a single polycistronic transcript (34, 35), but the zebrafish miR-430 cluster has many more miRNAs than reported in other clusters. The miR-430 miRNAs are conserved and clustered in other fish genomes, including *Fugu rubripes* and *Tetraodon nigroviridis* (Fig. 5C). The miR-

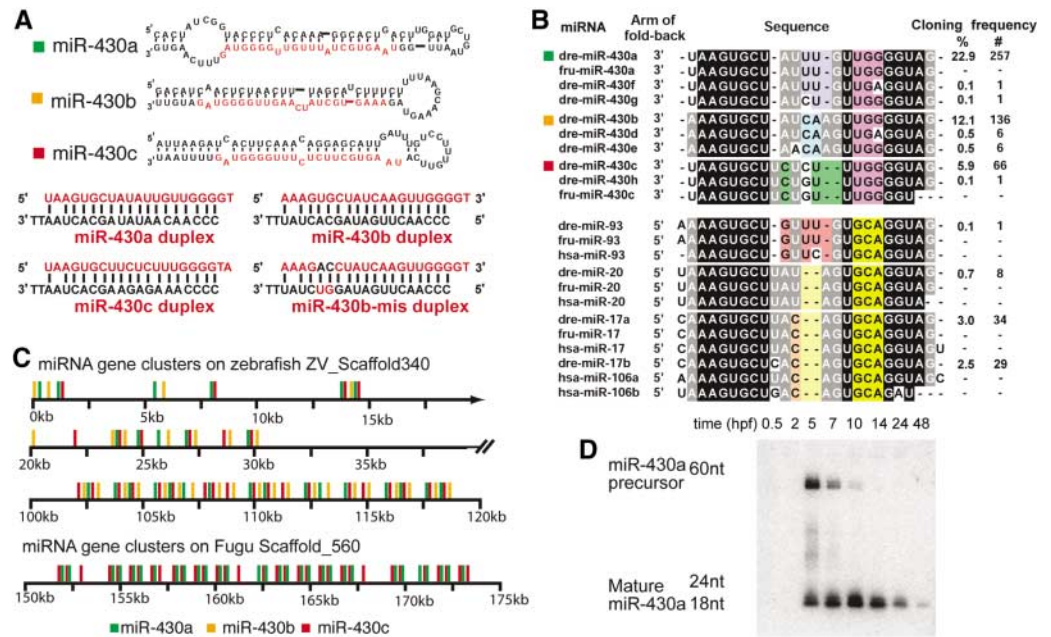
430 miRNAs belong to a superfamily that includes the vertebrate miR-17–miR-20 family, which are found in much smaller clusters in mammalian genomes (Fig. 5B). Despite the sequence similarities of the two families, members of the miR-17–miR-20 family derive from the opposite arm of their precursors, which suggest convergent rather than divergent origins of the two families. The miR-430 RNAs might share evolutionary origins with some of the miRNAs expressed specifically in mammalian embryonic stem cells (12), including miR-302 and miR-372, which have the same seed nucleotides and derive from the same arm of the hairpin.

The miR-430 miRNAs are initially expressed at about 50% epiboly [5 hours post-fertilization (hpf)], continue to be expressed during gastrulation and somitogenesis, and then decline at about 48 hpf (Fig. 5D) (25). Analysis of GFP sensors with perfect target sites for miR-430a or miR-430b suggested that the miR-430 miRNAs are ubiquitously expressed and active during early development (Fig. 2B) (25).

miR-430 Rescues Brain Morphogenesis in *MZdicer* Mutants

As described above, miRNA duplexes are still active in *MZdicer* mutants. This allowed us to determine if aspects of the *MZdicer* mutant phenotype could be suppressed by providing specific miRNAs that are normally expressed during early zebrafish development (miR-1, miR-204, miR-96, miR-203, miR-430a, miR-430b, or miR-430c). We also reasoned that such rescue would unequivocally demonstrate that a particular phenotype is caused by the loss of a specific mature miRNA and not by the lack of small interfering RNAs (siRNAs) or

Fig. 5. Identification of a highly expressed miRNA family. (A) Predicted hairpins of three miR-430 miRNAs together with the corresponding duplexes used for injection; mature miRNAs shown in red. miR-430b-mis contains two mismatches (black) in the 5' seed. (B) miR-430 miRNAs cloned from zebrafish (*dre*) and predicted in Fugu (*fru*) aligned with the miR-17-miR-20 family of human (*hsa*) miRNAs. (C) Color-coded representation of a miR-430 genomic cluster in the zebrafish and Fugu genomes. Each bar represents a predicted miRNA hairpin. (D) Northern blot analysis of the expression profile of miR-430a in wild-type embryos at different developmental stages.



the abnormal accumulation of pre-miRNAs in *MZdicer* mutants (5, 7, 20). We found that injection of miR-430 duplexes (miR-430a, miR-430b, or miR-430c) rescued the brain morphogenesis defects in *MZdicer* mutants (Figs. 3D and 4, C and G). This rescue was specific, as indicated by two control experiments. First, injection of unrelated miRNA duplexes did not cause any rescue (fig. S11) (25). Second, injection of a miRNA duplex with two point substitutions in the 5' seed did not rescue the *MZdicer* phenotype (miR-430b-mis; Figs. 4, D and H, and 5A; fig. S11). Rescue of *MZdicer* mutant embryos by normal brain ventricles and brain constrictions (Fig. 4, D and G, and fig. S11). For example, the midbrain-hindbrain boundary formed in *MZdicer*^{+miR-430} as in wild-type embryos (Fig. 4G and fig. S11). Injection of miR-430 also induced a substantial rescue of the neuronal defects observed in *MZdicer* mutants (fig. S7). *MZdicer*^{+miR-430} also displayed partially rescued gastrulation, retinal development, somite formation, and touch response (Figs. 3D and 4C and fig. S8). In contrast, the defects in the development of the ear and heart and the lack of circulation were not rescued (Fig. 3D and fig. S10). Later during development (90 hpf), *MZdicer*^{+miR-430} embryos were developmentally delayed and displayed reduced growth similar to *MZdicer*. These results indicate that loss of miR-430 miRNAs accounts for some but not all of the defects observed in *MZdicer* embryos.

Our study of zebrafish that lack Dicer RNaseIII activity and mature miRNAs provides three major insights into the roles of miRNAs during embryogenesis. First, our results suggest that mature miRNAs do not

have widespread essential roles in fate specification or signaling during early zebrafish development. Phenotypic comparison between *MZdicer* mutants and embryos with aberrant signaling pathways (Nodal, Hedgehog, Wnt, Notch, CXCR4, FGF, BMP, retinoic acid, or STAT3) suggests that none of these pathways is markedly affected by the absence of miRNAs (36). For example, *MZdicer* mutants do not display the phenotypes seen upon an increase or decrease in Nodal or BMP signaling. This suggests that miRNAs might have modulating or tissue-specific rather than obligatory roles in various signaling pathways. Similarly, our study reveals that *MZdicer* mutants can differentiate multiple cell types during development. This suggests that mature miRNAs are not required to specify the major embryonic cell lineages in zebrafish. Our results do not exclude more specific roles in fate specification, such as modulating the choice between highly related cell fates. For example, *lisy-6* in *Caenorhabditis elegans* controls the distinction between two closely related neurons, and mouse miR-181 seems to regulate the ratio of cell types within the lymphocyte lineage (18, 37). miRNAs might also function at later stages to stabilize and maintain a particular fate. For instance, miRNAs might repress large numbers of target mRNAs to maintain tissue homeostasis by dampening fluctuations in gene expression (38, 39). However, our transplantation results argue against an absolute requirement for miRNAs in every cell type. In particular, we generated fertile adults from *MZdicer* mutant donors by germ cell transplantation (fig. S1). This indicates that primordial germ cells, the ultimate stem cells, proliferate and remain pluripotent to form the adult germ line in the

absence of miRNAs. Multigeneration transplantation studies are required to determine if the lack of miRNAs has effects on germ cell maintenance (40, 41). More exhaustive analysis of different cell types and signaling pathways is needed to test for more subtle or later roles of miRNAs in zebrafish, but our current study excludes a general role in signaling, embryonic fate specification, or germ line stem cell development.

Second, our results suggest important roles for miRNAs during embryonic morphogenesis and differentiation, ranging from epiboly and somitogenesis to heart, ear, and neural development. For example, loss of Dicer leads to defects in the positioning of neurons, the defasciculation of axons, and impaired touch-induced behaviors. Most notably, mutants form a neural rod but fail to generate normal brain ventricles. In addition, the morphological constrictions that subdivide the anterior-posterior axis do not form in the absence of Dicer, despite the regionalization observed by marker analysis. These results reveal essential roles of miRNAs during zebrafish morphogenesis.

Third, our study identifies a previously unknown miRNA family, the absence of which is likely to account for the brain morphogenesis defects in *MZdicer* mutants. The miR-430 family has more genes than any miRNA family described to date, is conserved in fish, and is part of a superfamily found in other vertebrates. Injection of miR-430 duplexes suppresses the brain morphogenesis defects in *MZdicer* mutants. This complementation approach can now be applied to determine which miRNAs (or siRNAs) account for the *MZdicer* phenotypes that cannot be rescued by miR-430. The miR-430 family might inhibit mRNAs

that are provided maternally or expressed during early embryogenesis but are detrimental to later steps in morphogenesis. Cell shape changes, cell rearrangements, and fluid dynamics are thought to generate both extrinsic and intrinsic forces that contribute to neural tube and ventricle formation, but the underlying molecular mechanisms are poorly understood (42). The study of the miR-430 family and its targets therefore provides a genetic entry point to dissect the molecular basis of brain morphogenesis.

References and Notes

- D. P. Bartel, *Cell* **116**, 281 (2004).
- V. Ambros, *Nature* **431**, 350 (2004).
- G. Meister, T. Tuschl, *Nature* **431**, 343 (2004).
- A. Grishok *et al.*, *Cell* **106**, 23 (2001).
- G. Hutvagner *et al.*, *Science* **293**, 834 (2001).
- Y. Lee *et al.*, *Nature* **425**, 415 (2003).
- E. Bernstein, A. A. Caudy, S. M. Hammond, G. J. Hannon, *Nature* **409**, 363 (2001).
- B. P. Lewis, C. B. Burge, D. P. Bartel, *Cell* **120**, 15 (2005).
- E. Berezhikov *et al.*, *Cell* **120**, 21 (2005).
- J. M. Thomson, J. Parker, C. M. Perou, S. M. Hammond, *Nat. Methods* **1**, 47 (2004).
- J. H. Mansfield *et al.*, *Nat. Genet.* **36**, 1079 (2004).
- H. B. Houbaviy, M. F. Murray, P. A. Sharp, *Dev. Cell* **5**, 351 (2003).
- B. P. Lewis, I. H. Shih, M. W. Jones-Rhoades, D. P. Bartel, C. B. Burge, *Cell* **115**, 787 (2003).
- M. Kiriakidou *et al.*, *Genes Dev.* **18**, 1165 (2004).
- B. John *et al.*, *PLoS Biol.* **2**, e363 (2004).
- M. N. Poy *et al.*, *Nature* **432**, 226 (2004).
- S. Yekta, I. H. Shih, D. P. Bartel, *Science* **304**, 594 (2004).
- C. Y. Chen, L. Li, H. F. Lodish, D. P. Bartel, *Science* **303**, 83 (2004).
- E. Bernstein *et al.*, *Nat. Genet.* **35**, 215 (2003).
- C. Kanellopoulou *et al.*, *Genes Dev.* **19**, 489 (2005).
- E. Wienholds, M. J. Koudijs, F. J. van Eeden, E. Cuppen, R. H. Plasterk, *Nat. Genet.* **35**, 217 (2003).
- B. Ciruna *et al.*, *Proc. Natl. Acad. Sci. U.S.A.* **99**, 14919 (2002).
- L. P. Lim, M. E. Glasner, S. Yekta, C. B. Burge, D. P. Bartel, *Science* **299**, 1540 (2003).
- W. P. Kloosterman, E. Wienholds, R. F. Ketting, R. H. Plasterk, *Nucleic Acids Res.* **32**, 6284 (2004).
- A. J. Giraldez *et al.*, data not shown.
- Q. Liu *et al.*, *Science* **301**, 1921 (2003).
- N. Doi *et al.*, *Curr. Biol.* **13**, 41 (2003).
- Y. S. Lee *et al.*, *Cell* **117**, 69 (2004).
- J. W. Pham, J. L. Pellino, Y. S. Lee, R. W. Carthew, E. J. Sontheimer, *Cell* **117**, 83 (2004).
- Y. Tomari *et al.*, *Cell* **116**, 831 (2004).
- Materials and methods are available as supporting material on *Science* Online.
- M. E. Glasner *et al.*, in preparation.
- J. G. Doench, P. A. Sharp, *Genes Dev.* **18**, 504 (2004).
- Y. Lee *et al.*, *EMBO J.* **23**, 4051 (2004); published online 16 September 2004 (10.1038/sj.emboj.7600385).
- S. Baskerville, D. P. Bartel, *RNA* **11**, 241 (2005).
- A. F. Schier, *Curr. Opin. Genet. Dev.* **11**, 393 (2001).
- R. J. Johnston, O. Hobert, *Nature* **426**, 845 (2003).
- D. P. Bartel, C. Z. Chen, *Nat. Rev. Genet.* **5**, 396 (2004).
- L. P. Lim *et al.*, *Nature* **433**, 769 (2005).
- M. A. Blasco *et al.*, *Cell* **91**, 25 (1997).
- T. Fukagawa *et al.*, *Nat. Cell Biol.* **6**, 784 (2004).
- L. A. Lowery, H. Sive, *Mech. Dev.* **121**, 1189 (2004).
- We thank T. Tuschl and S. Pfeffer for help during the initial phase of the project; E. Wienholds and R. Plasterk for *Zdicer* mutants; and C. Antonio, B. Ciruna, G. Fishell, V. Greco, S. Mango, T. Schell, W. Talbot, A. Teleman, and D. Yelon for providing helpful comments on the manuscript. A.J.G. was supported by The European Molecular Biology Organization and is currently supported by The International Human Frontier Science Program Organization fellowship. S.M.H. is a General Motors Cancer Research Foundation Scholar. A.F.S. is an Irma T. Hirsch Trust Career Scientist and an Established Investigator of the American Heart Association. This work was also supported by grants from the NIH (A.F.S. and D.P.B.).

Supporting Online Material

www.sciencemag.org/cgi/content/full/1109020/DC1

Materials and Methods

Figs. S1 to S11

References

22 December 2004; accepted 25 February 2005

Published online 17 March 2005;

10.1126/science.1109020

Include this information when citing this paper.

REPORTS

The Optical Resonances in Carbon Nanotubes Arise from Excitons

Feng Wang,^{1*} Gordana Dukovic,^{2*} Louis E. Brus,² Tony F. Heinz^{1†}

Optical transitions in carbon nanotubes are of central importance for nanotube characterization. They also provide insight into the nature of excited states in these one-dimensional systems. Recent work suggests that light absorption produces strongly correlated electron-hole states in the form of excitons. However, it has been difficult to rule out a simpler model in which resonances arise from the van Hove singularities associated with the one-dimensional bond structure of the nanotubes. Here, two-photon excitation spectroscopy bolsters the exciton picture. We found binding energies of ~400 millielectron volts for semiconducting single-walled nanotubes with 0.8-nanometer diameters. The results demonstrate the dominant role of many-body interactions in the excited-state properties of one-dimensional systems.

Coulomb interactions are markedly enhanced in one-dimensional (1D) systems. Single-walled carbon nanotubes (SWNTs) provide an ideal model system for studying these effects. Strong electron-electron interactions are associated with many phenomena in the charge transport of SWNTs, including Coulomb blockade (1, 2),

Kondo effects (3, 4), and Luttinger liquid behavior (5, 6). The effect of Coulomb interactions on nanotube optical properties has remained unclear, in spite of its central importance both for a fundamental understanding of these model 1D systems (7–9) and for applications (7, 10, 11). Theoretical studies suggest that optically produced electron-hole pairs should, under their mutual Coulomb interaction, form strongly correlated entities known as excitons (12–18). Although some evidence of excitons has emerged from studies of nanotube optical spectra (7, 19) and excited-state dynamics (20), it is difficult to rule out an alternative

and widely used picture that attributes the optical resonances to van Hove singularities in the 1D density of states (21–23). Here, we demonstrate experimentally that the optically excited states of SWNTs are excitonic in nature. We measured exciton binding energies that represent a large fraction of the semiconducting SWNT band gap. As such, excitonic interactions are not a minor perturbation as in comparable bulk semiconductors, but actually define the optical properties of SWNTs. The importance of many-body effects in nanotubes derives from their 1D character; similar excitonic behavior is also seen in organic polymers with 1D conjugated backbones (24).

We identified excitons in carbon nanotubes using two-photon excitation spectroscopy. Two-photon transitions obey selection rules distinct from those governing linear excitation processes and thereby provide complementary insights into the electronic structure of excited states, as has been demonstrated in studies of molecular systems (25) and bulk solids (26). In 1D materials like SWNTs, the exciton states show defined symmetry with respect to reflection through a plane perpendicular to the nanotube axis. A Rydberg series of exciton states describing the relative motion of the electron and hole, analogous to the hydrogenic states, is then formed with definite parity with respect to this reflection plane. The even states are denoted as 1s, 2s, 3s, and so on, and the odd wave functions are labeled as 2p, 3p, and so on (27). Because of the weak spin-

¹Departments of Physics and Electrical Engineering,
²Department of Chemistry, Columbia University, 538 West 120th Street, New York, NY 10027, USA.

*These authors contributed equally to this work.

†To whom correspondence should be addressed.
E-mail: tony.heinz@columbia.edu

MicroRNAs Regulate Brain Morphogenesis in Zebrafish

Antonio J. Giraldez, Ryan M. Cinalli, Margaret E. Glasner, Anton J. Enright, J. Michael Thomson, Scott Baskerville, Scott M. Hammond, David P. Bartel and Alexander F. Schier

Science **308** (5723), 833-838.
DOI: 10.1126/science.1109020 originally published online March 17, 2005

ARTICLE TOOLS

<http://science.sciencemag.org/content/308/5723/833>

SUPPLEMENTARY MATERIALS

<http://science.sciencemag.org/content/suppl/2005/05/05/1109020.DC1>

REFERENCES

This article cites 39 articles, 11 of which you can access for free
<http://science.sciencemag.org/content/308/5723/833#BIBL>

PERMISSIONS

<http://www.sciencemag.org/help/reprints-and-permissions>

Use of this article is subject to the [Terms of Service](#)

Science (print ISSN 0036-8075; online ISSN 1095-9203) is published by the American Association for the Advancement of Science, 1200 New York Avenue NW, Washington, DC 20005. 2017 © The Authors, some rights reserved; exclusive licensee American Association for the Advancement of Science. No claim to original U.S. Government Works. The title *Science* is a registered trademark of AAAS.